

Diffusion of oxygen in uranium dioxide: A first-principles investigationFlorence Gupta,^{1,*} Alain Pasturel,² and Guillaume Brillant¹¹IRSN, DPAM, SEMIC, LETR, Saint Paul Lez Durance, France²Laboratoire de Physique et Modélisation des Milieux Condensés, CNRS, Maison des Magistères,
25 Avenue des Martyrs, BP 166, 38042 Grenoble, France

(Received 1 November 2009; revised manuscript received 17 December 2009; published 20 January 2010)

Results of *ab initio* density-functional theory calculations of the migration energies of oxygen vacancies and interstitials in stoichiometric UO_2 are reported. The diffusion of oxygen vacancies in UO_2 is found to be highly anisotropic, and the $[1\ 0\ 0]$ direction is energetically favored. The atomic relaxations play an important role in reducing the migration barriers. Within the generalized gradient approximation (GGA), we find that the migration energies of the preferred vacancies and interstitials paths are, respectively, 1.18 and 1.09 eV. With the inclusion of the Hubbard U parameter to account for the $5f$ electron correlations in GGA+ U , the vacancy migration energy is lowered to 1.01 eV while the interstitial migration energy increases slightly to 1.13 eV. We find, however, that the correlation effects have a drastic influence on the mechanism of interstitial migration through the stabilization of Willis-type clusters. Indeed, in contrast to GGA, in GGA+ U there is an inversion of the migration path with the so-called “saddle-point” position being lower in energy than the usual starting position. Thus while the migration barriers are nearly the same in GGA and GGA+ U , the mechanisms are completely different. Our results clearly indicate that both vacancies and interstitials contribute almost equally to the diffusion of oxygen in UO_2 .

DOI: [10.1103/PhysRevB.81.014110](https://doi.org/10.1103/PhysRevB.81.014110)

PACS number(s): 66.30.H-, 61.72.J-, 61.82.Ms

I. INTRODUCTION

The ceramic UO_2 is the most employed fuel material in nuclear reactors. To analyze the safety of nuclear reactors, which is the main concern of IRSN (Institut de Radioprotection et Sûreté Nucléaire) we need an understanding of this fuel in a number of possible accidental scenarios. We are concerned here with the accidental oxidation of the fuel for which it has been shown that the first step is governed by the diffusion of oxygen.¹ Thus the investigations concerning the diffusion mechanisms of oxygen in UO_2 are of crucial importance in nuclear reactor safety. The experimental determination of the migration energies of the oxygen vacancies and interstitials has been made but the interpretation of the experimental data is difficult. From these experiments, the migration energies of both vacancies and interstitials were found to lie in the range of 0.5–1.0 eV (Refs. 2–5) but the dominant mechanism has not yet been clearly established. Catlow⁶ found from atomistic simulations that vacancies diffuse faster than interstitials, and were the primary species contributing to the diffusion of oxygen. However, these simulations were based on empirical interatomic potentials assuming UO_2 to be a completely ionic compound. However, UO_2 is an antiferromagnetic semiconductor with a band gap of ~ 1.8 eV,⁷ and the bonding in this compound is not ionic but rather ionocovalent. The electronic structure of this material is known to be complex, and the density-functional theory (DFT) calculations in both the local-density and the generalized gradient (GGA) approximations yield a metallic ground state,^{8–10} in contradiction to experiments. This is due to an incorrect treatment of the $5f$ electrons that are not completely localized. The inclusion of the Hubbard parameter U to account for the correlation effects for the $5f$ electrons is necessary to obtain the correct band gap for this compound.^{11–13} Moreover, we showed in a previous paper¹³

that this parameter has an influence on the relative stability of structural defects in UO_2 . Considering this complexity in UO_2 , and the fact that DFT-based calculations on the formation energies of defects in UO_2 have yielded substantially different results from those obtained from atomistic simulations based on empirical potential, we decided to investigate the mechanisms of oxygen migration in UO_2 in the framework of DFT calculations with both GGA and GGA+ U approximations.

The first-principles techniques have made enormous progress during the last few years, and have now come to a stage where reliable results concerning a variety of physical phenomena in materials science can be expected. This is especially true for the calculation of diffusion barriers in bulk and surfaces, including the oxides.^{14–16} This has motivated the present paper, and to our knowledge no *ab initio* electronic-structure calculation of the self-diffusion barriers in this technologically important compound have been performed. An important result of the present study is that the migration barriers for vacancy and interstitial diffusion are such that both should contribute to diffusion. This is in contrast to the current models⁶ where vacancy is assumed to be the dominant contributor to diffusion. We believe that these results are important for modeling the oxidation behavior of UO_2 .

II. COMPUTATIONAL DETAILS

A small and a large cubic supercell with, respectively, 12 and 96 atoms (primitive cubic cell of UO_2 and a 2 2 2 times the primitive cubic cell) have been chosen to examine the effect of the size of the supercell on migration energies. We will show that while the effect of the supercell size is small in the case of oxygen vacancies, the results are substantially different for the case of oxygen interstitials due to the atomic

relaxations of the interstitial and its surroundings.

For the vacancies, the small cubic supercell of volume a^3 , contained 11 atoms while the large supercell of volume $(2a)^3$, included 95 atoms, both having a vacancy in the tetrahedral site at the starting position. For the interstitials similarly the small supercell contained 13 atoms while the large supercell included 97 atoms, both having an interstitial oxygen atom in an octahedral site. The calculations were performed using the Vienna *ab initio* simulation package (VASP) with projector augmented wave derived potentials.^{17,18} The GGA calculations were carried out with the PW91 version of the exchange and correlation term as implemented in the VASP code. For the U atom the outer 14 electrons and for the O atom the outer six electrons were treated as valence electrons. The Monkhorst-Pack grid of special k points with a division of 11 11 11 for the small supercell (12 atoms) and 4 4 4 for the large supercell (96 atoms) was employed. An energy cutoff of 400 eV was employed in the present calculation with the large supercell. The total energies and magnetic moments converged to better than 1 meV and $0.01\mu_B$, respectively, and the residual forces on the atoms were less than 0.01 eV/Å. The calculations are converged and were found to be insensitive to a further increase in either the k grid or the energy cutoff. The lattice parameters for the GGA and the spin-polarized antiferromagnetic GGA+ U ($U=4.0$ eV) calculations were, respectively, 5.38 and 5.52 Å, as calculated in our previous work;¹³ they were obtained by minimization of the total energies and used for the calculation of the defect-formation energies in UO_2 . The latter were found to be in good agreement with the available experimental data,^{5,19,20} and other previous theoretical calculations.^{21–25} In particular our predictions agree well with the very recent DFT+ U treatments^{23,24} of strong correlations in UO_2 . The value of 4.0 eV for the Hubbard parameter U , as in our previous work¹³ reproduces the insulating properties of UO_2 .⁷ All our calculations were performed at constant volume to reflect the infinitely small point-defect concentration.

The migration energies can be calculated in two different ways. The first one is based on the so-called nudged elastic band (NEB) method.^{26–28} One provides the initial and the final positions of the moving defect and an initial guess of the minimum energy path (MEP). This method then determines the true MEP, and hence the true saddle-point barrier for atomic migration. This method is very accurate and extremely useful for determining the migration paths and migration barriers in complex systems,^{26–28} for instance, in catalysis where it is hard to predict a good starting guess.²⁸ The NEB method is, however, demanding both in terms of computer time and memory, especially for large supercells. In the present case, we are interested in atomic diffusion in clearly defined directions, and the saddle-point position is expected to be situated roughly midway between the starting and the final positions of the moving defect. This allows us to propose an alternative method for determining the migration barriers. In this method, we calculate the total energies by relaxing all the atoms including the defect in both the starting position and the saddle-point position, and the difference of the two yields the migration barrier. In the NEB method, we divide the trajectory between the starting point and the

final point in a number of intermediate positions, and calculate the total energies for fully relaxed atomic positions. A comparison of the migration barriers from the two methods can then be made.

III. RESULTS AND DISCUSSION

We first discuss the results for the migration of oxygen vacancies obtained in GGA. The calculations were performed in three crystallographic directions, namely $[1\ 0\ 0]$, $[1\ 1\ 1]$, and $[1\ 1\ 0]$. UO_2 crystallizes in the fluorite-type structure. In the smaller supercell of volume a^3 the U atoms are located at the fcc sites $(0\ 0\ 0)$, $(0.5\ 0.5\ 0.0)$ and the oxygen atoms at the tetrahedral sites $(0.25\ 0.25\ 0.25)$. All coordinates are in cartesian system and expressed in terms of the cubic lattice parameter a of UO_2 . For the migration in the $[1\ 0\ 0]$ direction, the vacancy is moved from its initial position at $(0.25\ 0.25\ 0.25)$ to its final position $(0.75\ 0.25\ 0.25)$. The saddle point is expected to be located midway between the two at or around the position $(0.50\ 0.25\ 0.25)$. We have included three intermediate positions, including the saddle point, between the initial and final positions in our calculations using the NEB method. The results are shown in Fig. 1 for both the nonrelaxed and the fully relaxed atomic configurations. The relaxation energy of the initial or the final position is very small, ~ 0.04 eV. We see that the saddle point lies midway between the initial and the final positions and that the atomic relaxations play an important role since they lower the saddle-point energy by ~ 0.88 eV. We obtain identical results for the saddle-point energy calculated with and without NEB. However, for intermediate configurations the behavior is different; without the NEB method the moving atom might return to the closest initial or final position. This shows that in the present case one can safely calculate the migration barriers from the difference of the total energies with or without the NEB method. However this does not hold for intermediate configurations. For the vacancy migration in the $[1\ 0\ 0]$ direction, we obtain a migration energy of 1.47 eV with the smaller supercell (11 atoms) as shown in Fig. 1 where we also see that the migration barrier would be much higher, ~ 2.35 eV, without the inclusion of the atomic relaxations. These results are also summarized in Table I. Initially the migrating oxygen atom is surrounded by four U atoms in a tetrahedral environment at a distance of $\sim 0.433a$. But as it migrates this environment changes and at the saddle-point position $(0.5\ 0.25\ 0.25)a$, it has only two U atoms as nearest neighbors but at a much closer distance of $0.353a$. In the relaxation process the atom at the saddle-point position remains intact at its initial ideal position since it is symmetrically placed with respect to the two vacant sites. However, all U and O atoms around it experience some relaxation.

The results for oxygen-vacancy migration in the $[1\ 1\ 1]$ direction calculated in GGA for the smaller supercell are also shown in Fig. 1. The oxygen vacancy was displaced from the initial position $(0.25\ 0.25\ 0.25)a$ to the final position $(0.75\ 0.75\ 0.75)a$, and three intermediate positions were used in the calculation with the NEB method. The saddle-point position in this case falls at the center of the cube at $(0.50\ 0.50$

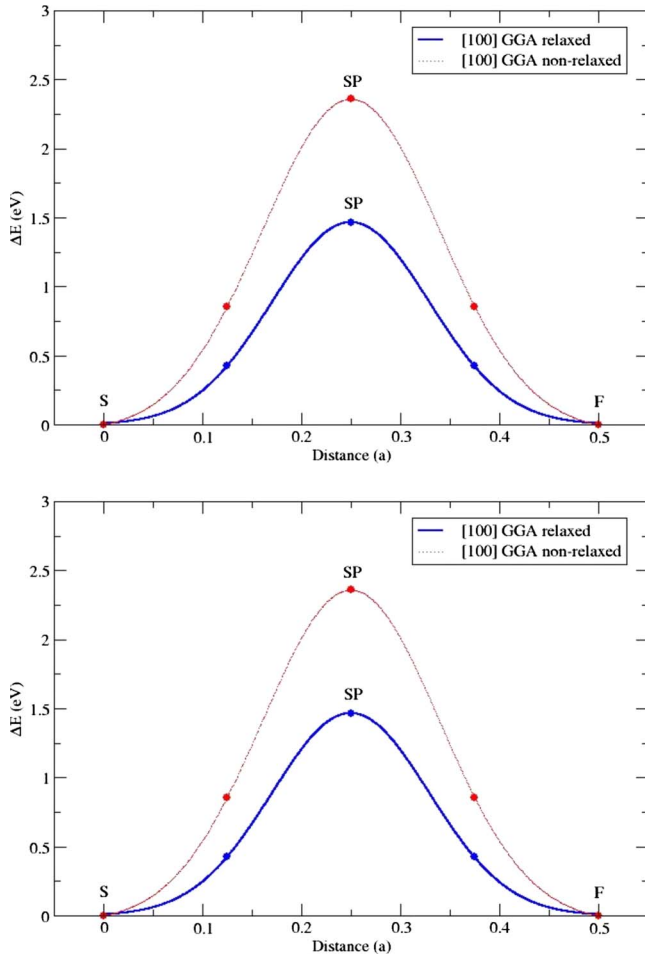


FIG. 1. (Color online) The migration paths for the oxygen-vacancy migration in [1 0 0] (upper panel) and [1 1 1] (lower panel) directions. The red (upper) curves indicate the results with the non-relaxed atomic positions and the blue (lower) curves are with the relaxed ones. The values at initial positions are taken as the origin of energy for both nonrelaxed and relaxed atomic configurations. The symbols S, F, and SP represent, respectively, the starting, final, and saddle-point positions.

0.50) *a*. A migration barrier of ~ 3.30 eV is obtained when atomic relaxations are included but a higher barrier of ~ 4.25 eV is obtained without relaxations. Since the saddle point is extremely symmetric, neither the saddle-point position nor the U atom positions are disturbed and the relaxation occurs only at the six surrounding oxygen sites which move away by ~ 0.17 Å from their initial positions.

The most important relaxations are found for the vacancy migration in the [1 1 0] direction from the initial site (0.25 0.25 0.25) *a* to the final site (0.75 0.75 0.25) *a* in which the saddle point is initially situated at (0.50 0.50 0.25) *a*, and again three intermediate positions were used in the NEB method. This saddle point is very unfavorable for the migrating oxygen atom since it is at a very short distance of $a/4$ from the U atom. One therefore expects a very high migration barrier. This is indeed the case when no atomic relaxations are included where one finds a migration barrier of 19.8 eV. However, the migrating atom exerts strong forces on the neighboring U and O atoms and counteracting forces are

TABLE I. Migration energies (eV) of an oxygen vacancy in the [1 0 0], [1 1 1], and [1 1 0] directions calculated within the GGA and GGA+*U* approximations with 11 atoms and 95 atoms supercells [of volume a^3 and $(2a)^3$, respectively] with nonrelaxed and fully relaxed atomic configurations.

| | GGA | | GGA+ <i>U</i> (<i>U</i> =4.0 eV) | |
|-------------------------------|------------|---------|-----------------------------------|---------|
| | Nonrelaxed | Relaxed | Nonrelaxed | Relaxed |
| Vacancy migration energy (eV) | | | | |
| [1 0 0] (11 atoms) | 2.35 | 1.47 | 2.31 | 1.02 |
| [1 0 0] (95 atoms) | 2.31 | 1.18 | 3.65 | 1.01 |
| [1 1 1] (11 atoms) | 4.25 | 3.30 | 4.17 | 3.04 |
| [1 1 1] (95 atoms) | 4.57 | 3.14 | 5.04 | 2.71 |
| [1 1 0] (11 atoms) | 19.80 | 2.12 | 18.31 | 2.39 |
| [1 1 0] (95 atoms) | 19.94 | 2.73 | 18.68 | 2.45 |

also exerted on the moving atom. There is a significant displacement of this atom, and the neighboring U and O atoms are displaced in such a way that the nearest U atom is now at a distance of ~ 2 Å from it. It also has now four more U atoms at a distance of $\sim a/2$. The other tetrahedral oxygen atoms no longer have a regular environment, and the lattice is fully perturbed. It leads to a dramatic decrease in the migration barrier to a very low value of ~ 2.12 eV with the NEB method. We obtain the same results at the saddle point without the NEB method for this case.

We now discuss the results for vacancy migration using the small supercell, within the GGA+*U* approach, in the same three directions considered above. As we mentioned previously, UO₂ is an antiferromagnetic insulator and an insulating gap can be obtained only within the GGA+*U* approximation. We have shown in our recent work¹³ that with a value of *U*=4.0 eV, the experimental band-gap value of ~ 1.8 eV can be obtained. This value also yielded the oxygen Frenkel pair formation energy in good agreement with experiment.^{5,19} We have therefore employed this value in the present work to investigate the effect of *f* electron correlations on the migration energies. The lattice parameter was kept fixed at $a=5.52$ Å, as obtained in GGA+*U* approximation. We obtain in the [1 0 0] direction a migration energy of 2.13 eV for the nonrelaxed atomic positions which is quite close to the value obtained above in the GGA for the nonrelaxed case. But the migration barrier is lowered to ~ 1.02 eV when the atomic relaxations are included. This is nearly ~ 0.45 eV lower than the value obtained in GGA. For the [1 1 1] and [1 1 0] directions, for both nonrelaxed and relaxed configurations, the values found with GGA+*U* are quite close to those obtained with GGA, as shown in Table I. In the relaxed configuration, the migration barriers are found to be 3.04 and 2.39 eV, respectively. The magnetic interactions appear to play a small role in vacancy diffusion. As one can see from Table I, both GGA and GGA+*U* calculations show that the oxygen vacancy migration is strongly anisotropic.

In order to examine the effect of cell size on oxygen-vacancy diffusion, we have performed calculations with the larger 2 2 2 supercell containing 95 atoms and an oxygen

TABLE II. Migration energies (eV) of an oxygen interstitial in the direct and interstitialcy mechanisms calculated within the GGA and GGA+ U approximations with 13 atoms and 97 atoms $U_{32}O_{65}$ cubic supercells [of volume a^3 and $(2a)^3$, respectively] with nonrelaxed and fully relaxed atomic configurations.

| Cubic cells | GGA | | GGA+ U ($U=4.0$ eV) | |
|---|------------|---------|------------------------|---------|
| | Nonrelaxed | Relaxed | Nonrelaxed | Relaxed |
| Direct interstitial migration energy (eV) | | | | |
| 13 atoms | 11.18 | 5.42 | 7.63 | 2.86 |
| 97 atoms | 11.18 | 3.51 | 6.41 | 2.14 |
| Interstitialcy migration energy (eV) | | | | |
| 13 atoms | 1.26 | 0.36 | 0.73 | -0.68 |
| 97 atoms | 1.16 | 1.09 | 0.48 | -1.13 |

vacancy using the NEB method with one image. As shown in Table I, the result obtained in GGA in the $[1\ 0\ 0]$ direction with this larger supercell for the nonrelaxed configuration, ~ 2.31 eV, is in good agreement with the value of ~ 2.35 eV obtained above with the small supercell. However, the value for the relaxed configuration ~ 1.18 eV, is smaller by ~ 0.3 eV than the one with the smaller supercell. With the GGA+ U approximation, we obtain a value of ~ 1.01 eV for the migration energy in the relaxed configuration in the $[1\ 0\ 0]$ direction, in good agreement with the value ~ 1.02 eV obtained above with the smaller supercell. As shown in Table I, the vacancy migration energies in the $[1\ 1\ 1]$ and $[1\ 1\ 0]$ directions obtained with the larger supercell are quite close to those obtained with the smaller supercell in both GGA and GGA+ U approximations. The only exception is the value of the migration energy in the $[1\ 1\ 0]$ direction in GGA where the difference between the small and large supercell results is ~ 0.6 eV. This is of course a special direction since here the relaxation effects are particularly strong. Our results thus show that the cell size plays only a small role in vacancy migration. We should also note from Table I that inclusion of correlation effects generally lowers the migration barrier by ~ 0.2 – 0.4 eV, depending on the cell size and the direction of migration.

These conclusions cannot be extended to the case of interstitial migration where not only the results are found to be significantly different with the larger supercell but the inclusion of correlation effects affects the migration behavior drastically. This probably reflects in a certain manner the effect of Willis-type clusters²⁹ in interstitial diffusion. Two different kinds of interstitial mechanisms have been considered, a direct migration and an interstitialcy mechanism. For the direct migration of an interstitial oxygen atom in the $[1\ 1\ 0]$ direction, which is the only possible direction, we used a small supercell of volume a^3 . In this supercell the interstitial oxygen atom migrates from its initial position in the center of the cube at $(0.50\ 0.50\ 0.50)a$ to the middle of an edge of the cube, and the “ideal” saddle point is placed at $(0.25\ 0.25\ 0.50)a$. Both the initial and saddle-point positions were relaxed and we obtained a large value of ~ 5.42 eV for the migration energy in the GGA, as shown in Table II. This is due to the strong repulsive interaction at the saddle point

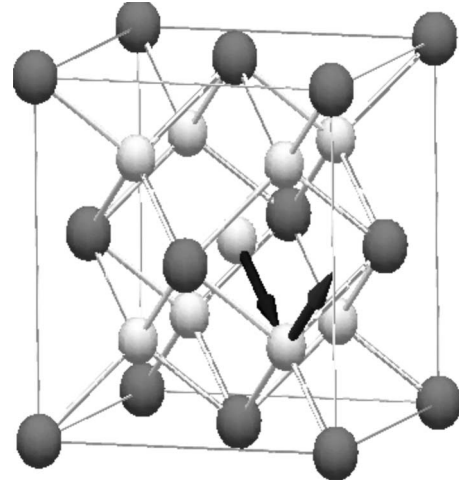


FIG. 2. A schematic representation of the interstitialcy mechanism for the oxygen interstitial diffusion in the fluorite structure cubic cell. The U atoms are shown in dark gray and the O atoms in light gray. The arrows indicate the correlated migration of the interstitial oxygen atom located initially at the center of the cube to the tetrahedral site and the migration of the tetrahedral oxygen to the neighboring octahedral interstitial site.

between the migrating atom and the closest uranium atoms located at a distance of $\sim 0.354a$. With the larger supercell containing 97 atoms, a much reduced barrier of ~ 3.51 eV is obtained. Within GGA+ U , the difference between the large-cell value, ~ 2.14 eV, and the small-cell value, ~ 2.86 eV, is much smaller despite the fact that relaxation effects remain strong in both cases. In any case, these are rather strong barriers for interstitial migration through direct hopping.

The interstitialcy mechanism, shown in Fig. 2, in which the interstitial atom diffuses in a correlated manner with a tetrahedral oxygen atom, is known to be the easiest for interstitial diffusion.⁶ This is also found in our calculations. We included one intermediate position between the initial and the final positions with the NEB method in the GGA. The interstitial diffusion occurs from the initial octahedral site $(0.50\ 0.50\ 0.50)$ to the final octahedral site $(0.00\ 1.00\ 0.50)$ with the help of the tetrahedral oxygen at $(0.25\ 0.75\ 0.75)$, where all coordinates given here are in units of the lattice parameter a of the small cubic cell. In contrast to the case of vacancy migration where the effect of relaxations is small, ~ 0.04 eV in the starting position, the relaxations play a major role in interstitial diffusion via the interstitialcy mechanism. Without the inclusion of the atomic relaxations, a migration barrier of ~ 1.26 eV is obtained with the interstitialcy mechanism. However, the energy is lowered by ~ 0.89 eV in the initial position due to atomic relaxations but the energy lowering is far higher, ~ 1.79 eV, in the saddle-point position, resulting in a net barrier of only ~ 0.36 eV for interstitial migration with the interstitialcy mechanism. The calculations were repeated without the NEB method also and the same results were obtained for the saddle-point energy.

With the larger supercell containing 97 atoms, the calculations were performed with one intermediate position between the initial and the final positions of the interstitial

atom with the interstitialcy mechanism in GGA. Without relaxations we obtain a migration barrier of 1.16 eV which is close to the value obtained with the smaller 13 atoms supercell, as shown in Table II. The energy lowering of 1.78 eV, due to the relaxations in the saddle-point position is also practically the same as obtained with the smaller supercell. However, the energy lowering is far higher, 1.71 eV, in the initial starting position with the larger supercell. This results in a much higher migration energy of 1.09 eV, for the interstitialcy mechanism. The large energy lowering in the initial position, 1.71 eV, arises from the formation of Willis-type clusters as discussed below in the framework of the GGA+ U approximation.

For the large cell with 97 atoms we obtained, in the GGA+ U approximation, an energy barrier of ~ 0.48 eV for the nonrelaxed configurations. This migration barrier is expected to be considerably modified by relaxations as we saw above. Here the relaxation energies are quite large. In the starting position there is an energy lowering of ~ 2.43 eV which is larger than the relaxation energy obtained above in the GGA. What is surprising, however, is the huge energy lowering of ~ 4.03 eV at the saddle-point position. This results in a migration energy, as shown in Table II, that is negative with a value of ~ -1.13 eV. The negative sign indicates that the so-called “saddle-point position” is more stable than the “starting position” in the GGA+ U approximation and the role of the two interchanged, meaning that the interstitial migration will occur the other way around. The value of the migration barrier, ~ 1.13 eV, obtained in the present work is nearly the same as obtained in the GGA but this is a pure coincidence given the completely different nature of relaxations in the two frameworks. The value of the migration barrier obtained with the smaller supercell of volume a^3 is also given in Table II for completeness.

A close examination of the atomic displacements shows that the saddle point in the relaxed configuration is located at the positions (0.296 0.296 0.301) and (0.456 0.456 0.298), all expressed in terms of the lattice parameter $2a$ of the large cell. These correspond to the positions (0.6 0.6 0.6) and (0.4 0.4 0.6) when expressed in terms of the lattice parameters of

the regular small cell. These positions are quite close to those given by Willis *et al.*²⁹ The binding energy of this cluster, ~ 1.13 eV, obtained in the present work agrees quite well with the one deduced by Ruello *et al.*³⁰ experimentally. Similar clusters are also formed at practically the same positions at the saddle point in GGA but they are not stable since in this case the saddle point is a true saddle point.

IV. CONCLUSIONS

In summary, our *ab initio* electronic-structure calculations have shown that in UO_2 the vacancy migration is extremely anisotropic and occurs preferentially in the [1 0 0] direction. The migration energies obtained with the larger supercell within the GGA approximation for both vacancies and interstitials are rather close, 1.18 eV for vacancies and 1.09 eV for interstitials with the interstitialcy mechanism. The inclusion of electronic correlations for the $5f$ electrons at the U sites lowers the vacancy migration energy to 1.01 eV. The interstitial migration mechanism is drastically modified by the inclusion of correlation effects which stabilize the Willis-type clusters at the saddle-point configuration and become the ground state of the system. The normal saddle point is no longer the true saddle point but serves instead the departing point for the migrating oxygen interstitials. The migration energy, ~ 1.13 eV, obtained in this case is, fortuitously, quite close to the GGA value. These results are within the range of the values obtained experimentally. In the irradiation environment, the defects are produced due to the irradiation-induced atomic displacements, and hence the defect migration is the controlling mechanism for diffusion. From our results we can conclude that both vacancies and interstitials contribute almost equally to diffusion. We hope that this work will stimulate more experimental investigations in this technologically important compound.

ACKNOWLEDGMENTS

The work presented in this paper was partly supported by EDF (Electricité de France).

*Corresponding author. Present address: Institut de Radioprotection et Sûreté Nucléaire, 92 Fontenay-aux-Roses, France; florence.gupta@irsn.fr

¹S. Aronson, R. Roof, and J. Belle, *J. Chem. Phys.* **27**, 137 (1957).

²A. Auskern and J. Belle, *J. Nucl. Mater.* **3**, 267 (1961).

³K. C. Kim and D. R. Olander, *J. Nucl. Mater.* **102**, 192 (1981).

⁴G. E. Murch, *Diffus. Defect Data* **32**, 9 (1983).

⁵H. Matzke, *J. Chem. Soc., Faraday Trans. 2* **83**, 1121 (1987).

⁶C. R. A. Catlow, *Proc. R. Soc. London, Ser. A* **353**, 533 (1977).

⁷J. Schoenes, *Phys. Rep.* **63**, 301 (1980).

⁸T. Petit, B. Morel, C. Lemaignan, A. Pasturel, and B. Bigot, *Philos. Mag. B* **73**, 893 (1996).

⁹J. P. Crocombette, F. Jollet, L. Thien Nga, and T. Petit, *Phys. Rev. B* **64**, 104107 (2001).

¹⁰M. Freyss, T. Petit, and J. P. Crocombette, *J. Nucl. Mater.* **347**, 44 (2005).

¹¹S. L. Dudarev, D. Nguyen Mann, and A. P. Sutton, *Philos. Mag. B* **75**, 613 (1997).

¹²R. Laskowski, G. K. H. Madsen, P. Blaha, and K. Schwarz, *Phys. Rev. B* **69**, 140408(R) (2004).

¹³F. Gupta, G. Brilliant, and A. Pasturel, *Philos. Mag.* **87**, 2561 (2007).

¹⁴L. Tsetseris, A. Kalfagiannis, S. Logothetidis, and S. T. Pantelides, *Phys. Rev. Lett.* **99**, 125503 (2007).

¹⁵C. Tang, B. Tuttle, and R. Ramprasad, *Phys. Rev. B* **76**, 073306 (2007).

¹⁶A. S. Foster, A. Shluger, and R. M. Nieminen, *Phys. Rev. Lett.* **89**, 225901 (2002).

¹⁷G. Kresse and D. Joubert, *Phys. Rev. B* **59**, 1758 (1999).

- ¹⁸G. Kresse and J. Furthmuller, *Comput. Mater. Sci.* **6**, 15 (1996).
- ¹⁹R. Clausen, W. Hayes, J. E. Macdonald, R. Osborn, and M. T. Hutchings, *Phys. Rev. Lett.* **52**, 1238 (1984).
- ²⁰H. J. Matzke, *J. Chem. Soc., Faraday Trans. II* **86**, 1243 (1990).
- ²¹H. Y. Geng, Y. Chen, Y. Kaneta, M. Iwasawa, T. Ohnuma, and M. Kinoshita, *Phys. Rev. B* **77**, 104120 (2008).
- ²²D. A. Andersson, T. Watanabe, C. Deo, and B. P. Uberuaga, *Phys. Rev. B* **80**, 060101(R) (2009).
- ²³B. Dorado, B. Amadon, M. Freyss, and M. Bertolus, *Phys. Rev. B* **79**, 235125 (2009).
- ²⁴F. Jollet, G. Jomard, B. Amadon, J. P. Crocombette, and D. Torumba, *Phys. Rev. B* **80**, 235109 (2009).
- ²⁵P. Nerikar, T. Watanabe, J. S. Tulenko, S. R. Phillpot, and S. B. Sinnott, *J. Nucl. Mater.* **384**, 61 (2009).
- ²⁶G. Henkelman, B. P. Uberuaga, and H. J. Jonsson, *J. Chem. Phys.* **113**, 9901 (2000).
- ²⁷G. Henkelman and H. J. Jonsson, *J. Chem. Phys.* **113**, 9978 (2000).
- ²⁸G. Henkelman and H. J. Jonsson, *Phys. Rev. Lett.* **86**, 664 (2001).
- ²⁹B. T. M. Willis, *Proc. Br. Ceram. Soc.* **1**, 9 (1964); B. J. M. Bevan, J. E. Grey, and B. T. M. Willis, *J. Solid State Chem.* **61**, 1 (1986); A. D. Murray and B. T. M. Willis, *ibid.* **84**, 52 (1990).
- ³⁰P. Ruello, G. Chirlesan, G. Petot-Evras, C. Petot, and L. Desgranges, *J. Nucl. Mater.* **325**, 202 (2004).